Low-dissipation model of three-terminal refrigerator: performance bounds and comparative analyses

OPEN ACCESS
IOP Publishing
Journal of Physics A: Mathematical and Theoretical
J. Phys. A: Math. Theor. **55** (2022) 065001 (19pp)
https://doi.org/10.1088/1751-8121/ac47b0

Low-dissipation model of three-terminal refrigerator: performance bounds and comparative analyses

Zhexu Li[1], Julian Gonzalez-Ayala[2,3], Hanxin Yang[1], Juncheng Guo[1,*] and A Calvo Hernández[2,3]

[1] College of Physics and Information Engineering, Fuzhou University, Fuzhou 350116, People's Republic of China
[2] Departamento de Física Aplicada, Universidad de Salamanca, 37008 Salamanca, Spain
[3] Instituto Universitario de Física Fundamental y Matemáticas (IUFFyM), Universidad de Salamanca, 37008 Salamanca, Spain

E-mail: jcguo@fzu.edu.cn

Received 18 November 2021, revised 20 December 2021
Accepted for publication 4 January 2022
Published 19 January 2022

Abstract

In the present paper, a general non-combined model of three-terminal refrigerator beyond specific heat transfer mechanisms is established based on the low-dissipation assumption. The relation between the optimized cooling power and the corresponding coefficient of performance (COP) is analytically derived, according to which the COP at maximum cooling power (CMP) can be further determined. At two dissipation asymmetry limits, upper and lower bounds of CMP are obtained and found to be in good agreement with experimental and simulated results. Additionally, comparison of the obtained bounds with previous combined model is presented. In particular it is found that the upper bounds are the same, whereas the lower bounds are quite different. This feature indicates that the claimed universal equivalence for the combined and non-combined models under endoreversible assumption is invalid within the frame of low-dissipation assumption. Then, the equivalence between various finite-time thermodynamic models needs to be reevaluated regarding multi-terminal systems. Moreover, the correlation between the combined and non-combined models is further revealed by the derivation of the equivalent

*Author to whom any correspondence should be addressed.

condition according to which the identical upper bounds and distinct lower bounds are theoretically shown. Finally, the proposed non-combined model is proved to be the appropriate model for describing various types of thermally driven refrigerator. This work may provide some instructive information for the further establishments and performance analyses of multi-terminal low-dissipation models.

Keywords: finite-time cycle, low-dissipation model, three-terminal refrigerator, performance bounds, comparative analyses

(Some figures may appear in colour only in the online journal)

1. Introduction

The primary task of thermodynamics is to analyze and optimize the performance of thermodynamic devices. In the light of quasi-static assumption, Carnot efficiency and Carnot coefficients of performance (COPs), which are the universal upper bounds of efficiency and COPs for heat engines, heat pumps, and refrigerators, have been derived. Nevertheless, quasi-static assumption implies infinite cycle time and zero power output and cooling (heating) power. As a consequence, these universal upper bounds are of great theoretical significance but the practical implications are limited.

Concerning this issue, the more realistic thermodynamic cycles with finite power are desired, which gave rise to the birth and development of a branch of thermodynamics, i.e. finite-time thermodynamics. Inspired by the pioneering work of Curzon and Ahlborn [1], endoreversible model provides a valuable approach to study the behaviors of practical thermodynamic devices. Besides, linear and minimally nonlinear irreversible thermodynamics models have been put forward and developed in the past decades [2–4]. Particularly, in 2010 Esposito *et al* [5] proposed a unified model of Carnot heat engine beyond specific heat transfer mechanisms by assuming the irreversible entropy generation of heat exchanging process is inversely proportional to the time duration of the process with a dissipation coefficient (low-dissipation assumption). The validity of low-dissipation model has been proven for a wide class of thermodynamic devices and a wide range of heat transfer laws [5–16].

By means of the proposed various finite-time thermodynamic models, the performance characteristics of two-terminal thermodynamic devices, mainly including heat engine [17–22], chemical engine [10], refrigerator [6, 11–14, 23], have been intensively investigated. Specifically, the performances of the abovementioned devices at maximum power [5, 7, 9, 17–19] and several trade-off functions, e.g. arbitrary power [20, 21], efficient power [22], arbitrary cooling power [23], Chi function [11, 14, 24], and Omega function [25–28], have been discussed, respectively. Notably, the bounds of efficiency and COP at different figures of merit fitting well with realistic devices have been derived based on low-dissipation models [5, 6, 12, 14, 24]. More importantly, some consistent results have been derived with different finite-time thermodynamic models [3, 5, 7, 10, 16, 29–32], which led to the thriving discussions about the internal correlations and equivalence between the existing finite-time thermodynamic models, e.g. minimally nonlinear irreversible models [3, 29], endoreversible models [16, 30–32], and low-dissipation models.

In addition to two-terminal devices, multi-terminal systems play the increasingly important roles in the utilization and control of low-grade thermal energy [33, 34] and the energy resources at microscopic scale [35, 36]. However, in the previous studies, the applications of

the low-dissipation assumption focused on two-terminal systems. The low-dissipation multi-terminal models and the associated performance research have been still absent since the publication of reference [5]. In this regard, Guo *et al* established a combined low-dissipation model of three-terminal refrigerator by coupling a low-dissipation heat engine and a low-dissipation refrigerator and investigated its performance for the first time [37]. After that, Ye *et al* further develop the combined low-dissipation three-terminal refrigerator model [38].

Regarding the low-dissipation model of multi-terminal system, there are still several important issues needed to be addressed: (i) Is there another approach to construct the low-dissipation model of three-terminal refrigerator? (ii) Whether the low-dissipation three-terminal models with different arrangements are equivalent and lead to the same performance bounds? (iii) Whether the proved equivalence between endoreversible and low-dissipation models for two-terminal devices is still valid for three-terminal system? (iv) What kind of arrangement is the most appropriate one that can be used to describe different thermally driven refrigerators?

We will address the above issues in this work. First, a non-combined low-dissipation model of three-terminal refrigerator will be established. Secondly, the performance characteristics of the low-dissipation three-terminal refrigerator will be investigated with special emphasis on the performance bounds of COP at maximum cooling power (CMP). Thirdly, by comparing the obtained exchanging heats, irreversible entropy generations, and performance bounds with reference [37], the difference and correlation between the combined and non-combined models will be revealed. Accordingly, the general equivalence between these two arrangements within the frame of endoreversible assumption is shown to be no longer valid. Furthermore, the equivalence condition for the combined and non-combined models under low-dissipation assumption will be explicitly given. Finally, the appropriate arrangement which could be used to describe thermally driven refrigerators of different nature is analyzed. Accordingly, the paper is structured as follow. Section 2 contains the proposed model for the non-combined model. Sections 3 and 4 show the optimum performance regimes and the influences of the main involved parameters, respectively. Upper and lower bounds of CMP are specifically analyzed in section 5. A detailed and comparative study for the combined and non-combined low-dissipation models is presented in section 6. Finally, section 7 contains some valuable conclusions and future prospects.

2. Model description

The model of a three-terminal Carnot refrigerator operating among high-temperature heat reservoir, environment, and cooled space with temperatures T_{H}, T_{O}, and T_{C} respectively, is shown schematically in figure 1, where Q_{H}, Q_{O}, and Q_{C} are, respectively, the heats exchanged between the refrigerator and three heat reservoirs during the three isothermal processes. A class of heat-driven refrigerators, e.g. absorption, adsorption, and ejector refrigerators can be described by using the above three-terminal model from the viewpoint of thermodynamics [37]. At reversible limit, one has $Q_{\mathrm{Hr}} = T_{\mathrm{H}}\Delta S_{\mathrm{H}}$, $Q_{\mathrm{Cr}} = T_{\mathrm{C}}\Delta S_{\mathrm{C}}$, and $Q_{\mathrm{Or}} = T_{\mathrm{O}}\Delta S_{\mathrm{O}}$. ΔS_{H}, ΔS_{C}, and ΔS_{O} are the reversible entropy changes in the corresponding isothermal processes. According to the second law of thermodynamics, the relation between the reversible entropy changes can be obtained as

$$\Delta S_{\mathrm{H}} + \Delta S_{\mathrm{C}} = \Delta S_{\mathrm{O}}. \tag{1}$$

The COP at reversible limit are given by [39]

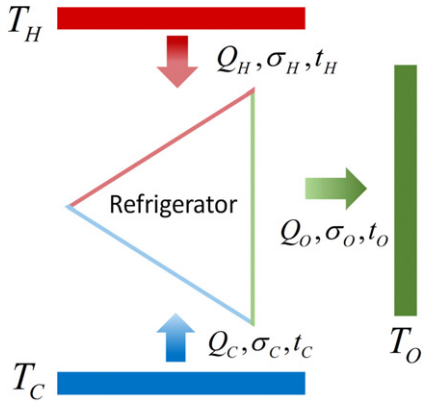

Figure 1. Schematic diagram of a three-terminal refrigerator model working among three heat sources with temperatures $T_{\rm H}$, $T_{\rm O}$, and $T_{\rm C}$.

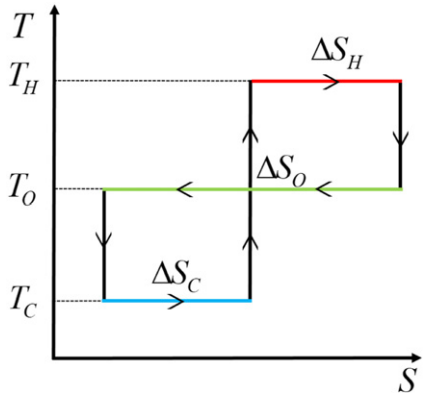

Figure 2. $T-S$ diagram of a reversible ejector refrigerator.

$$\psi_{\rm r} = \frac{T_{\rm C}(T_{\rm H} - T_{\rm O})}{T_{\rm H}(T_{\rm O} - T_{\rm C})}, \tag{2}$$

at which the corresponding cooling power is zero. The $T-S$ diagram of a reversible ejector refrigerator is shown in figure 2 as an example.

In order to obtain the COP of the three-terminal refrigerator at nonzero cooling power, irreversibilities are introduced in the heat-transfer processes by adopting low-dissipation assumption. Accordingly, the heats exchanged between the working fluid and the three reservoirs are given by [5, 7, 14]

$$Q_{\rm H} = Q_{\rm Hr}\left(1 - \frac{\sigma_{\rm H}}{t_{\rm H}}\right) = T_{\rm H}\Delta S_{\rm H}\left(1 - \frac{\sigma_{\rm H}}{t_{\rm H}}\right), \tag{3}$$

$$Q_{\rm C} = Q_{\rm Cr}\left(1 - \frac{\sigma_{\rm C}}{t_{\rm C}}\right) = T_{\rm C}\Delta S_{\rm C}\left(1 - \frac{\sigma_{\rm C}}{t_{\rm C}}\right), \tag{4}$$

and

$$Q_{\rm O} = Q_{\rm Or}\left(1+\frac{\sigma_{\rm O}}{t_{\rm O}}\right) = T_{\rm O}\Delta S_{\rm O}\left(1+\frac{\sigma_{\rm O}}{t_{\rm O}}\right), \tag{5}$$

where $t_{\rm H}$, $t_{\rm O}$, and $t_{\rm C}$ are the time durations of the three isothermal heat exchanging processes; $\sigma_{\rm H}$, $\sigma_{\rm C}$, and $\sigma_{\rm O}$ are the corresponding dissipation parameters containing all the information of irreversibilities. With the above expressions, the cooling power R and COP ψ of the system can be further expressed as

$$R = \frac{Q_{\rm C}}{\tau} = \frac{T_{\rm C}\Delta S_{\rm C}\left(1-\frac{\sigma_{\rm C}}{t_{\rm C}}\right)}{t_{\rm H}+t_{\rm O}+t_{\rm C}} \tag{6}$$

and

$$\psi = \frac{Q_{\rm C}}{Q_{\rm H}} = \frac{T_{\rm C}\Delta S_{\rm C}\left(1-\frac{\sigma_{\rm C}}{t_{\rm C}}\right)}{T_{\rm H}\Delta S_{\rm H}\left(1-\frac{\sigma_{\rm H}}{t_{\rm H}}\right)}, \tag{7}$$

where $\tau = t_{\rm H}+t_{\rm O}+t_{\rm C}$ is the whole cycle time of the three-terminal Carnot refrigerator by ignoring the time durations of the three adiabatic processes. Notably, the assumption of neglecting the time durations of adiabatic processes requires that the time durations of the adiabatic processes are much less than those of the heat-transfer processes in the cycle. However, this assumption cannot be valid for the quantum adiabatic process whose adiabatic time scale is quite large due to the degenerate energy levels [40]. Consequently, it is worth indicating that the adiabatic processes proposed in the present paper refer to the thermodynamic adiabatic processes in which the working substance is required to be thermally isolated. In addition, for quantum systems, the thermodynamic adiabatic processes should be considered as the sudden change of the Hamiltonian [41]. The rapidly changing conditions prevent the working substance from adapting its density of state, as a result, the adiabatic time scale can be ignored comparing to the heat-transfer processes. It can be realized from equations (3)–(7) that reversible condition can be recovered when $t_i \to \infty$ or $\sigma_i \to 0$ ($i = {\rm H}, {\rm C}, {\rm O}$), namely, $Q_{\rm H} \to Q_{\rm Hr}$, $Q_{\rm C} \to Q_{\rm Cr}$, $Q_{\rm O} \to Q_{\rm Or}$, $R \to 0$, and $\psi \to \psi_{\rm r}$.

It is worthy to indicate that the value of reversible entropy change is somewhat trivial and has no influence on the efficiency and COP for the low-dissipation two-terminal devices [5, 7, 13, 37]. Nevertheless, for the low-dissipation three-terminal refrigerator, the practical meanings of $\Delta S_{\rm H}$, $\Delta S_{\rm C}$, and $\Delta S_{\rm O}$ should be emphasized, i.e. the measure of the different component sizes inside the system [13, 24, 37]. Attending the above comments and equation (1), the associated dimensionless cooling power can be further defined as

$$\tilde{R} = R\frac{\sigma_{\rm H}+\sigma_{\rm O}+\sigma_{\rm C}}{T_{\rm O}\Delta S_{\rm O}} \tag{8}$$

by scaling according to the size of the system. Different from the low-dissipation two-terminal devices, the performances of the three-terminal refrigerator are dependent of the values of reversible entropy changes, as shown by equations (6)–(8).

In addition, by considering the practical meaning of reversible entropy change, the size ratio of different components should be kept constant for a given three-terminal refrigerator. Consequently, an important parameter accounting for the size ratio of different components

inside the three-terminal refrigerator is introduced as

$$A=\frac{\Delta S_{\mathrm{H}}}{\Delta S_{\mathrm{O}}}=\frac{\Delta S_{\mathrm{O}}-\Delta S_{\mathrm{C}}}{\Delta S_{\mathrm{O}}}=\frac{T_{\mathrm{O}}\left(1+\frac{\sigma_{\mathrm{O}}}{t_{\mathrm{O}}}\right)-T_{\mathrm{C}}\left(1-\frac{\sigma_{\mathrm{C}}}{t_{\mathrm{C}}}\right)}{T_{\mathrm{H}}\left(1-\frac{\sigma_{\mathrm{H}}}{t_{\mathrm{H}}}\right)-T_{\mathrm{C}}\left(1-\frac{\sigma_{\mathrm{C}}}{t_{\mathrm{C}}}\right)} \tag{9}$$

by using equations (1), (3)–(5), and the first law of thermodynamics. According to equations (1) and (9), the value of A should be limited in the region of $A_{\mathrm{r}}<A<1$, where $A_{\mathrm{r}}=(T_{\mathrm{O}}-T_{\mathrm{C}})/(T_{\mathrm{H}}-T_{\mathrm{C}})$ is the value of A at reversible limit ($t_i\to\infty$ ($i=\mathrm{H},\mathrm{C},\mathrm{O}$)).

3. Optimal relation between the cooling power and COP

From the above model, the optimal relations between the time durations of three heat-transferring processes by maximizing $\tilde{R}$ for given value of size ratio A can be derived by using equations (8) and (9), namely,

$$\tilde{t}_{\mathrm{H}}=\frac{A\tilde{\sigma}_{\mathrm{H}}\tilde{T}_{\mathrm{H}}+\sqrt{A\tilde{\sigma}_{\mathrm{H}}\tilde{\sigma}_{\mathrm{O}}\tilde{T}_{\mathrm{H}}}}{(-1+A)\frac{\tilde{\sigma}_{\mathrm{C}}}{\tilde{t}_{\mathrm{C}}}\tilde{T}_{\mathrm{C}}+\left(-1+\tilde{T}_{\mathrm{C}}-A\tilde{T}_{\mathrm{C}}+A\tilde{T}_{\mathrm{H}}\right)} \tag{10}$$

and

$$\tilde{t}_{\mathrm{O}}=\frac{\tilde{\sigma}_{\mathrm{O}}+\sqrt{A\tilde{\sigma}_{\mathrm{H}}\tilde{\sigma}_{\mathrm{O}}\tilde{T}_{\mathrm{H}}}}{(-1+A)\frac{\tilde{\sigma}_{\mathrm{C}}}{\tilde{t}_{\mathrm{C}}}\tilde{T}_{\mathrm{C}}+\left(-1+\tilde{T}_{\mathrm{C}}-A\tilde{T}_{\mathrm{C}}+A\tilde{T}_{\mathrm{H}}\right)}, \tag{11}$$

respectively. In equations (10) and (11), $\tilde{T}_{\mathrm{H}}=T_{\mathrm{H}}/T_{\mathrm{O}}$, $\tilde{T}_{\mathrm{C}}=T_{\mathrm{C}}/T_{\mathrm{O}}$, $\tilde{t}_{\mathrm{H}}=t_{\mathrm{H}}/(\sigma_{\mathrm{H}}+\sigma_{\mathrm{O}}+\sigma_{\mathrm{C}})$, $\tilde{t}_{\mathrm{C}}=t_{\mathrm{C}}/(\sigma_{\mathrm{H}}+\sigma_{\mathrm{O}}+\sigma_{\mathrm{C}})$, and $\tilde{t}_{\mathrm{O}}=t_{\mathrm{O}}/(\sigma_{\mathrm{H}}+\sigma_{\mathrm{O}}+\sigma_{\mathrm{C}})$ are respectively the dimensionless temperatures and time durations; $\tilde{\sigma}_{\mathrm{H}}=\sigma_{\mathrm{H}}/(\sigma_{\mathrm{H}}+\sigma_{\mathrm{O}}+\sigma_{\mathrm{C}})$, $\tilde{\sigma}_{\mathrm{O}}=\sigma_{\mathrm{O}}/(\sigma_{\mathrm{H}}+\sigma_{\mathrm{O}}+\sigma_{\mathrm{C}})$, and $\tilde{\sigma}_{\mathrm{C}}=\sigma_{\mathrm{C}}/(\sigma_{\mathrm{H}}+\sigma_{\mathrm{O}}+\sigma_{\mathrm{C}})$ are dimensionless dissipation parameters which also stand for the dissipation symmetry of the three-terminal refrigerator.

Substituting equations (10) and (11) into equations (7) and (8), the optimized cooling power and the corresponding COP as the functions of $\tilde{t}_{\mathrm{C}}$ and A can be derived as

$$\psi=\frac{(-1+A)\left(\tilde{\sigma}_{\mathrm{C}}-\tilde{t}_{\mathrm{C}}\right)\tilde{T}_{\mathrm{C}}\left(A\tilde{\sigma}_{\mathrm{H}}\tilde{T}_{\mathrm{H}}+\sqrt{A\tilde{\sigma}_{\mathrm{H}}\tilde{\sigma}_{\mathrm{O}}\tilde{T}_{\mathrm{H}}}\right)}{A\tilde{T}_{\mathrm{H}}\left[\tilde{\sigma}_{\mathrm{H}}\left(\tilde{t}_{\mathrm{C}}+\tilde{\sigma}_{\mathrm{C}}\tilde{T}_{\mathrm{C}}-A\tilde{\sigma}_{\mathrm{C}}\tilde{T}_{\mathrm{C}}-\tilde{t}_{\mathrm{C}}\tilde{T}_{\mathrm{C}}+A\tilde{t}_{\mathrm{C}}\tilde{T}_{\mathrm{C}}\right)+\tilde{t}_{\mathrm{C}}\sqrt{A\tilde{\sigma}_{\mathrm{H}}\tilde{\sigma}_{\mathrm{O}}\tilde{T}_{\mathrm{H}}}\right]} \tag{12}$$

and

$$\tilde{R}=\frac{(-1+A)\left(\tilde{\sigma}_{\mathrm{C}}-\tilde{t}_{\mathrm{C}}\right)\tilde{T}_{\mathrm{C}}\left[(-1+A)\tilde{\sigma}_{\mathrm{C}}\tilde{T}_{\mathrm{C}}+\tilde{t}_{\mathrm{C}}\left(-1+\tilde{T}_{\mathrm{C}}-A\tilde{T}_{\mathrm{C}}+A\tilde{T}_{\mathrm{H}}\right)\right]}{\tilde{t}_{\mathrm{C}}^{2}\left[\left(\tilde{\sigma}_{\mathrm{O}}-\tilde{t}_{\mathrm{C}}+\tilde{t}_{\mathrm{C}}\tilde{T}_{\mathrm{C}}-\tilde{\sigma}_{\mathrm{C}}\tilde{T}_{\mathrm{C}}\right)+2\sqrt{A\tilde{\sigma}_{\mathrm{H}}\tilde{\sigma}_{\mathrm{O}}\tilde{T}_{\mathrm{H}}}+A\left(\tilde{\sigma}_{\mathrm{C}}\tilde{T}_{\mathrm{C}}+\tilde{t}_{\mathrm{C}}\tilde{T}_{\mathrm{H}}-\tilde{t}_{\mathrm{C}}\tilde{T}_{\mathrm{C}}+\tilde{\sigma}_{\mathrm{H}}\tilde{T}_{\mathrm{H}}\right)\right]}, \tag{13}$$

respectively. Equation (12) shows that the COP is the function of the temperature, dissipation parameter, size ratio, and time duration. Besides, it can be deduced from equations (3)–(5) that the absolute values of the associated irreversible entropy production for the three heat-transfer processes can be expressed as $\Delta S_i\sigma_i/t_i$ ($i=\mathrm{H},\mathrm{C},\mathrm{O}$), respectively. Consequently, for the given values of temperature, dissipation parameter, and size ratio, the time duration, namely,

the irreversible entropy production plays the important role in determining the value of COP. More importantly, the optimal relation between $\tilde{R}$ and ψ for a three-terminal refrigerator with the given value of A can be further obtained by eliminating $\tilde{t}_C$ in equations (12) and (13). After a cumbersome algebra the obtained result can be read as

$$\tilde{R} = \frac{A_5 x^3 + A_6 x^2 + A_7 x}{A_8 x + A_9}, \tag{14}$$

where $x = (A_3 + A_4\psi) / (A_1 + A_2\psi)$ and the explicit expressions of A_i ($i = 1$–9) are given by equations (A1)–(A9) in appendix A. Equation (14) shows that the size ratio has great influence on the performance characteristics of the system, which will be discussed in detail in next section.

4. Performance optimum analyses

In this section the performance optimum results are analyzed in terms of the size ratio and the dissipation parameters.

4.1. The influence of size ratio A

According to equation (14), the parametric plots of the optimized cooling power and corresponding COP for the given values of A and at different dissipation limits are generated in figure 3. It can be seen from figure 3(a) that the variation of $\tilde{R}$ with ψ is parabolic for a given value of A. There exist a minimum and a maximum COP, i.e. $\psi_{\min,A}$ and $\psi_{\max,A}$ at which $\tilde{R} = 0$. Besides, the maximum cooling power $\tilde{R}_{\max,A}$ can be achieved when $\psi = \psi_{Rm,A}$. $\psi_{Rm,A}$ indicates not only the corresponding COP at maximum cooling power, but also the lower bound of the optimal operating region. Specifically, the low-dissipation three-terminal refrigerator with a given value of size ratio should be restricted to operate in the region of $\psi_{Rm,A} < \psi < \psi_{\max,A}$ due to the fact that one can always find the corresponding point with the same value of $\tilde{R}$ but higher value of ψ in the region of $\psi_{Rm,A} < \psi < \psi_{\max,A}$ comparing to the points outside. Accordingly, the associated time durations can be further deduced in the light of equations (10)–(12). In addition, the influence of dissipation symmetry on the optimal relation between $\tilde{R}$ and ψ can be realized from figure 3(b). The influence will be discussed in detail in subsection 4.2.

Figure 3(a) also shows that $\psi_{\min,A}$, $\psi_{\max,A}$, and $\psi_{Rm,A}$ all decrease as A grows monotonically. Nevertheless, $\tilde{R}_{\max,A}$ is not a monotonic function of A. The curves of $\psi_{Rm,A} - A$, $\tilde{R}_{\max,A} - A$, and $\tilde{R}_{\max,A} - \psi_{Rm,A}$ can be further plotted by using equation (14) and the numerical calculation, which are shown in figures 4 and 5. It can be found out from figure 4 that there exists an optimal value of size ratio A_{Rm} which makes $\tilde{R}_{\max,A}$ attain its maximum $\tilde{R}_{\max}$. The corresponding CMP ψ_{Rm} can be also determined from figures 4 and 5. Besides, figure 4 shows that the reversible regime, namely $\psi_{Rm,A} \to \psi_r$ and $\tilde{R}_{\max,A} \to 0$, can be approached at the limit of $A \to A_r$. In contrast, at the limit of $A \to 1$, one has $\psi_{Rm,A} \to 0$ and $\tilde{R}_{\max,A} \to 0$. This is a reasonable result since $A \to 1$ implies the size of the component contacting with cooled space is zero and the system is disabled. Attending the aforementioned characteristics, the size ratio of the three-terminal refrigerator should be designed in the region of $A_r < A < A_{Rm}$, within which the performance trade-off between cooling power and COP needs to be made. Notably, it can be also noticed that the optimal relation between the cooling power and COP for the low-dissipation three-terminal refrigerator, shown by figure 5, is similar to that of endoreversible three-terminal refrigerator [42–44], namely, both parabolic.

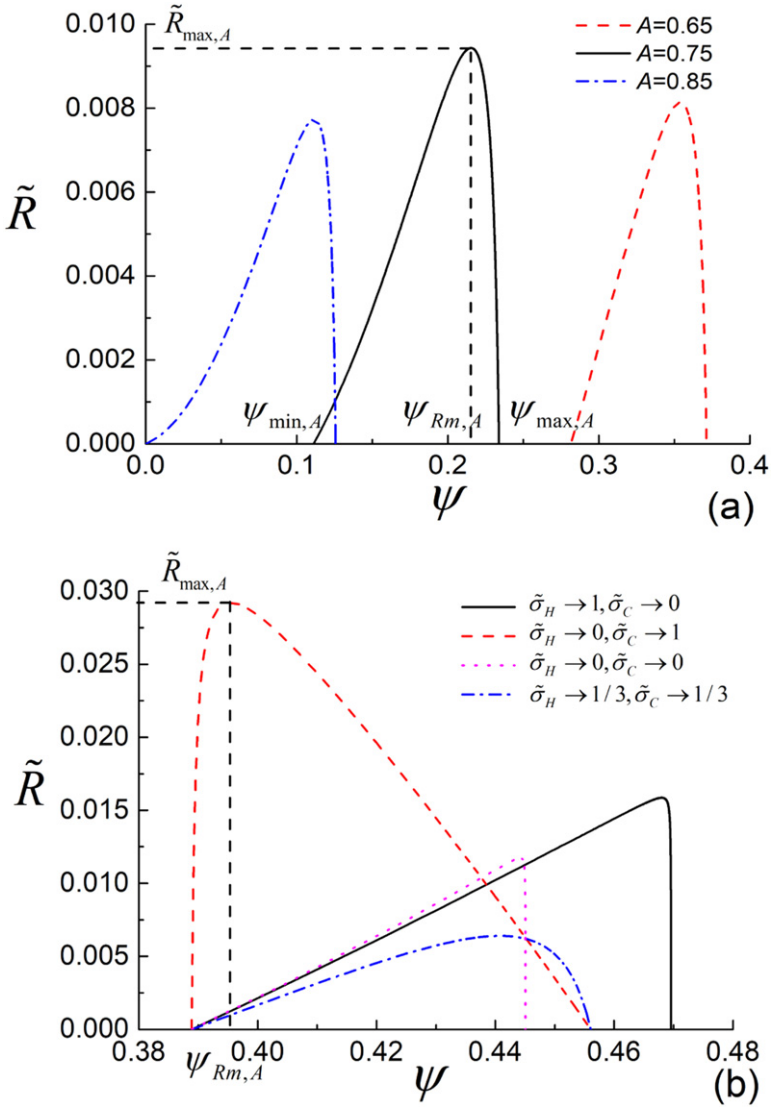

Figure 3. Behaviors of the optimized cooling power varying with the corresponding COP (a) for different values of A and (b) at different dissipation limits, where $\tilde{T}_{\rm H} = 1.2$, $\tilde{T}_{\rm C} = 0.8$, ($A_{\rm r} = 0.5$, $\psi_{\rm r} = 0.667$), (a) $\tilde{\sigma}_{\rm H} = \tilde{\sigma}_{\rm C} = 0.3$, $\tilde{\sigma}_{\rm O} = 0.4$, and (b) $A = 0.6$.

4.2. The influence of dissipative parameter σ

The curves of $\tilde{R}_{\max,A} - \psi_{Rm,A}$ in figure 5 also indicate that the value of ψ_{Rm} closely depends on the three dissipation parameters for given values of temperatures. The explicit behavior of ψ_{Rm} varying with $\tilde{\sigma}_{\rm H}$ and $\tilde{\sigma}_{\rm C}$ is given in figure 6 by means of equation (14) and the numerical calculation.

More importantly, it can be seen from figure 6 that the maximum and minimum values of ψ_{Rm} can be attained at two extreme dissipation asymmetry conditions, namely, $\tilde{\sigma}_{\rm H} \to 1$, $\tilde{\sigma}_{\rm C} \to 0$, $\tilde{\sigma}_{\rm O} \to 0$, and $\tilde{\sigma}_{\rm H} \to 0$, $\tilde{\sigma}_{\rm C} \to 1$, $\tilde{\sigma}_{\rm O} \to 0$, respectively. In other words, when all

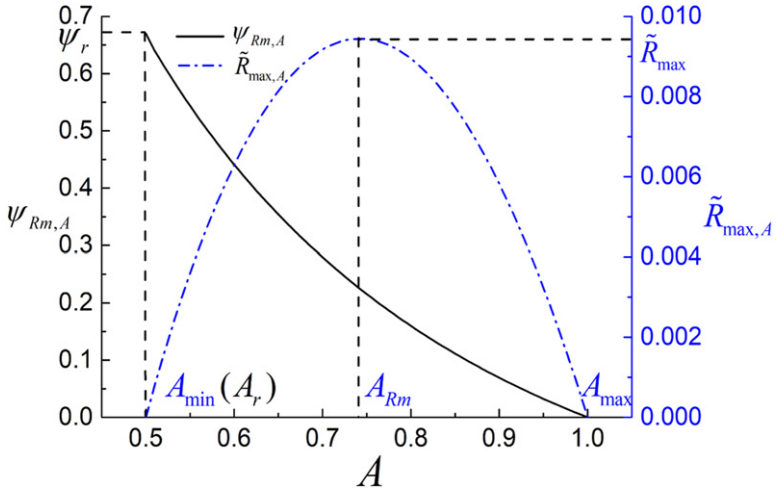

Figure 4. Variations of $\psi_{Rm,A}$ (black solid line) and $\tilde{R}_{\max,A}$ (blue dot-dashed line) with A; $\tilde{\sigma}_{\rm H} = \tilde{\sigma}_{\rm C} = 0.3$, $\tilde{\sigma}_{\rm O} = 0.4$, $\tilde{T}_{\rm H} = 1.2$, $\tilde{T}_{\rm C} = 0.8$ ($A_{\rm r} = 0.5$, $\psi_{\rm r} = 0.667$).

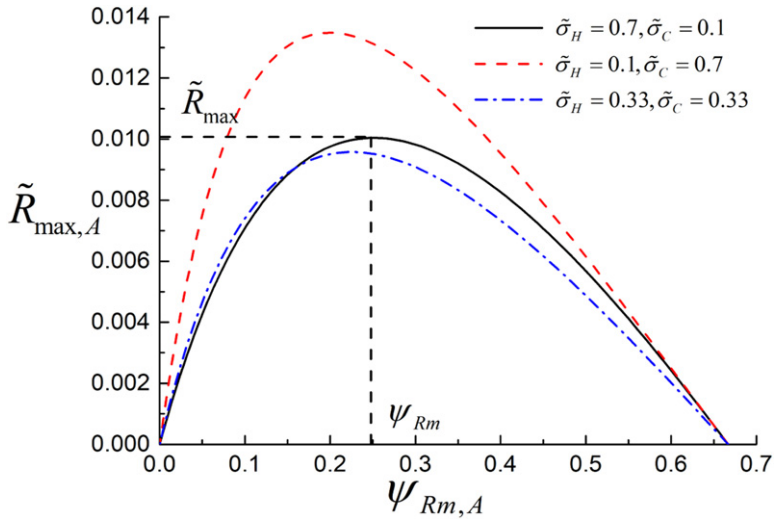

Figure 5. Behaviors of $\tilde{R}_{\max,A}$ versus the associated COP $\psi_{Rm,A}$ for different values of $\tilde{\sigma}_i$ ($i = {\rm H, C, O}$); $\tilde{T}_{\rm H} = 1.2$, $\tilde{T}_{\rm C} = 0.8$, and $\tilde{\sigma}_{\rm O} = 1 - \tilde{\sigma}_{\rm H} - \tilde{\sigma}_{\rm C}$.

the dissipation is generated from high-temperature terminal, ψ_{Rm} achieves its maximum. This characteristic is accordant with the combined low-dissipation three-terminal refrigerator model [37]. On the contrary, ψ_{Rm} reaches its minimum when the dissipation concentrates in low-temperature terminal, which is different from the result obtained in reference [37]. The insightful analyses for the difference between the combined model adopted in reference [37] and the model proposed in the present paper will be given in section 6.

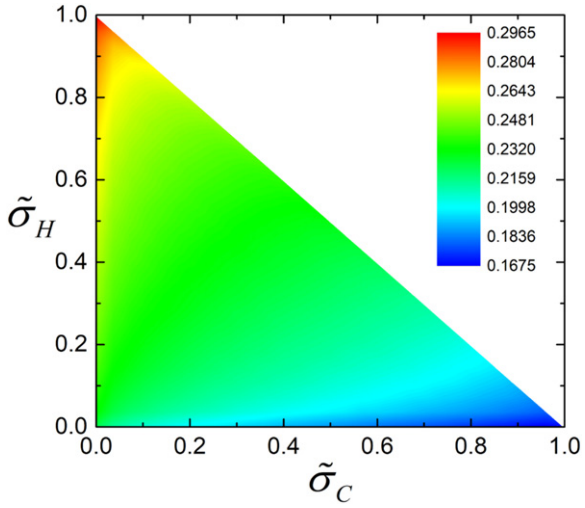

Figure 6. The three-dimensional projection of the CMP ψ_{Rm} varying with $\tilde{\sigma}_{\mathrm{H}}$ and $\tilde{\sigma}_{\mathrm{C}}$, where $\tilde{T}_{\mathrm{H}} = 1.2$, $\tilde{T}_{\mathrm{C}} = 0.8$, and $\tilde{\sigma}_{\mathrm{O}} = 1 - \tilde{\sigma}_{\mathrm{H}} - \tilde{\sigma}_{\mathrm{C}}$.

5. Upper and lower bounds

The above analyses lead to the significant achievement of the present paper. Namely, the three-dimensional upper and lower bounds of ψ_{Rm} varying with $\tilde{T}_{\mathrm{H}}$ and $\tilde{T}_{\mathrm{C}}$ can be numerically obtained by using the similar approaches and setting $\tilde{\sigma}_{\mathrm{H}} \to 1$, $\tilde{\sigma}_{\mathrm{C}} \to 0$, $\tilde{\sigma}_{\mathrm{O}} \to 0$, and $\tilde{\sigma}_{\mathrm{H}} \to 0$, $\tilde{\sigma}_{\mathrm{C}} \to 1$, $\tilde{\sigma}_{\mathrm{O}} \to 0$, respectively, which is shown in figure 7.

Besides, a series of experimental and simulated results reported in previous researches are collected to validate the proposed model and the obtained bounds. These reported results are listed in table 1 and denoted by the solid dots in figure 7. Notably, the bounded region is in accordance with most of the experimental and simulated results, which can be easily realized from table 1 and figure 7.

It is also noted that some of the reported COPs go out of the bounded region, which is due to the following reasons: (1) Carnot cycle is not usually adopted by the actual thermally driven refrigerators [34, 48, 52–54] because it needs a large volume ratio; (2) the thermally driven refrigerators may not be operated at the regime of maximum cooling power [53, 54] since the COP at maximum cooling power for a given value of size ratio is just the lower bound of the optimal operating region ($\psi_{Rm,A} < \psi < \psi_{\max,A}$) and, in consequence, the maximum COP and average COP are more concerned by the researchers from the engineering perspective; (3) the internal dissipation and external heat leakage losses are not taken into account in the present work, but they are inevitable in practice [48, 54]. In addition, it should be pointed out that the comparison between the experimental and simulated results and the obtained bounds is not a strict validation due to the abovementioned reasons. The comparison is aimed at showing the obtained bounds are of practical significance to some extent.

6. Comparative analyses with the combined low-dissipation model

One of the combined model of three-terminal refrigerator consisting of a Carnot refrigerator driven by a Carnot engine is shown by figure 8. It has been proved that the models shown

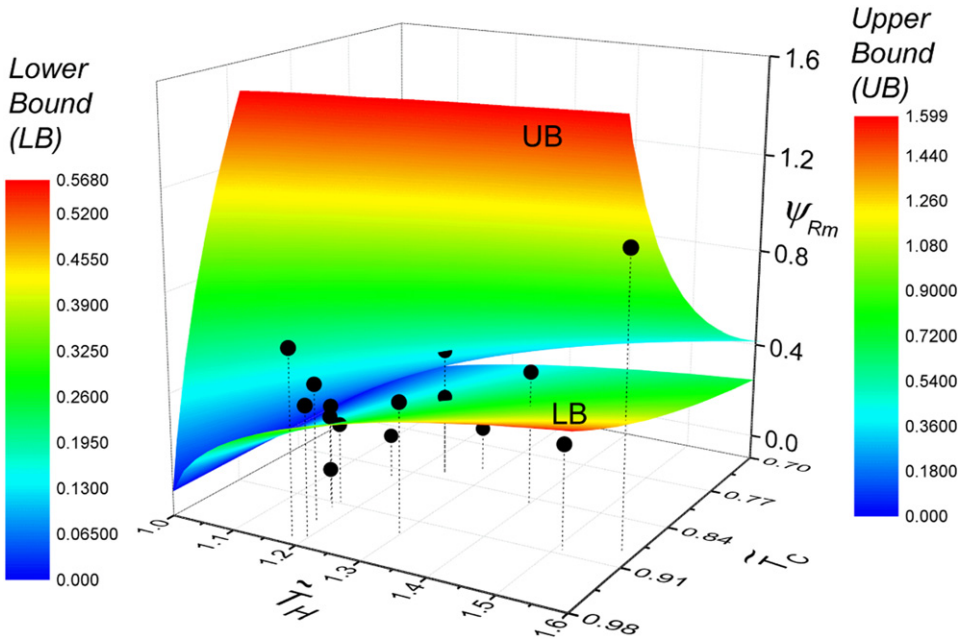

Figure 7. The three-dimensional graph of ψ_{Rm} varying with $\tilde{T}_{\mathrm{H}}$ and $\tilde{T}_{\mathrm{C}}$ and the reported COPs collected in table 1.

by figures 1 and 8 are equivalent within the framework of endoreversible assumption when Newton's law is adopted [42, 43, 55]. Comparing to the model proposed in the present paper, the time duration of the heat-transfer process contacting with intermediate-temperature terminal is divided into two parts in the combined model of the three-terminal refrigerator, namely $t_{\mathrm{O}} = t'_{\mathrm{OH}} + t'_{\mathrm{OC}}$. By adopting endoreversible assumption and Newton's law, the exchanged heats Q_{O}, Q'_{OH}, and Q'_{OC} in figures 1 and 8 can be expressed as

$$Q_{\mathrm{O}} = \alpha t_{\mathrm{O}}(T_{\mathrm{o}} - T_{\mathrm{O}}), \tag{15}$$

$$Q'_{\mathrm{OH}} = \alpha t'_{\mathrm{OH}}(T_{\mathrm{o}} - T_{\mathrm{O}}), \tag{16}$$

and

$$Q'_{\mathrm{OC}} = \alpha t'_{\mathrm{OC}}(T_{\mathrm{o}} - T_{\mathrm{O}}), \tag{17}$$

respectively, where α is the heat transfer coefficients between the working fluid and the intermediate-temperature reservoir, T_{o} is the associated temperature of the working fluid. It can be deduced from equations (15)–(17) that $Q_{\mathrm{O}} = Q'_{\mathrm{OH}} + Q'_{\mathrm{OC}}$. In addition, it can be further realized that the irreversible entropy productions of the related heat transfer processes for these two models are also the same by noticing

$$\frac{Q_{\mathrm{O}}}{T_{\mathrm{O}}} - \frac{Q_{\mathrm{O}}}{T_{\mathrm{o}}} = \frac{Q'_{\mathrm{OH}} + Q'_{\mathrm{OC}}}{T_{\mathrm{O}}} - \frac{Q'_{\mathrm{OH}} + Q'_{\mathrm{OC}}}{T_{\mathrm{o}}}. \tag{18}$$

Table 1. Reported COPs of various thermally driven refrigerators and the corresponding bounds of ψ_{Rm} for the low-dissipation three-terminal refrigerator model at given temperatures.

				Bounds of ψ_{Rm} from the present paper		
$\tilde{T}_C$	$\tilde{T}_H$	ψ_r	Reported COP	Upper	Lower	Inside the region (Y/N)
0.934	1.30	3.27	0.433 [33]	1.13	0.359	Y
0.830	1.24	0.945	0.230 [34]	0.416	0.211	Y
0.830	1.24	0.945	0.427 [34]	0.416	0.211	N
0.970	1.18	4.93	0.650 [45]	1.47	0.330	Y
0.850	1.40	1.62	0.450 [46]	0.673	0.309	Y
0.943	1.18	2.52	0.460 [47]	0.906	0.290	Y
0.853	1.18	0.885	0.0750 [48]	0.391	0.191	N
0.811	1.28	0.939	0.0770 [48]	0.419	0.219	N
0.967	1.20	4.88	0.430 [49]	1.49	0.340	Y
0.888	1.58	2.91	1.07 [50]	1.11	0.421	Y
0.918	1.17	1.63	0.320 [51]	0.638	0.245	Y
0.912	1.16	1.43	0.0400 [52]	0.573	0.228	N
0.912	1.16	1.43	0.260 [52]	0.573	0.228	Y
0.904	1.51	3.18	0.320 [53]	1.15	0.422	N
0.908	1.17	1.43	0.225 [54]	0.580	0.236	N

Consequently, the above discussions lead to the conclusion that the two models shown by figures 1 and 8, respectively, are generally equivalent under endoreversible assumption [42, 43, 55].

However, in the regime of low-dissipation assumption, the differences between these two models are prominent. Specifically, comparing the bounds of ψ_{Rm} shown in figure 7 and the bounds obtained based on the combined model [37], one can find out that the upper bounds are literally the same, whereas the lower bounds are completely different, which are shown in figures 9(a) and (b). The abovementioned difference indicates that the low-dissipation non-combined model proposed in the present paper and the low-dissipation combined model adopted in reference [37] are not equivalent anymore, which can be explained as follows.

According to low-dissipation assumption, the exchanged heats Q_O, Q'_{OH}, and Q'_{OC} in the non-combined and combined models shown by figures 1 and 8 are given by equation (5),

$$Q'_{OH} = T_O \Delta S'_{OH} \left(1 + \frac{\sigma'_{OH}}{t'_{OH}}\right), \tag{19}$$

and

$$Q'_{OC} = T_O \Delta S'_{OC} \left(1 + \frac{\sigma'_{OC}}{t'_{OC}}\right), \tag{20}$$

respectively. In equations (19) and (20), $\Delta S'_{OH}$ and $\Delta S'_{OC}$ are the entropy changes of two heat transfer processes at reversible limit, σ'_{OH} and σ'_{OC} are the corresponding dissipation parameters. The associated irreversible entropy productions of the above processes can be further obtained from equations (5), (19), and (20) as

$$\Delta S'_{OH,ir} = \frac{Q'_{OH}}{T_O} - \Delta S'_{OH} = \frac{\Delta S'_{OH}\sigma'_{OH}}{t'_{OH}}, \tag{21}$$

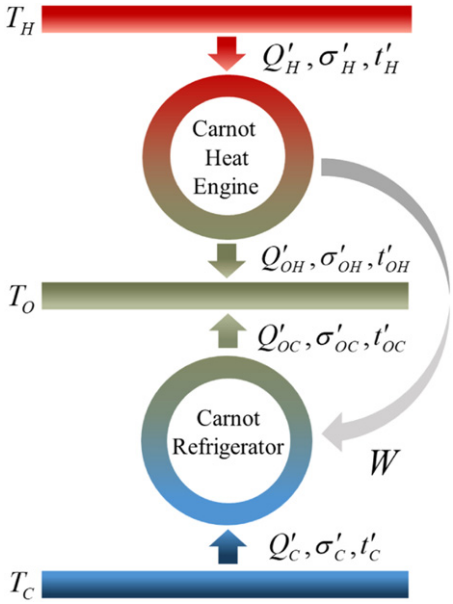

Figure 8. Combined model of the three-terminal refrigerator.

$$\Delta S'_{\mathrm{OC,ir}} = \frac{Q'_{\mathrm{OC}}}{T_{\mathrm{O}}} - \Delta S'_{\mathrm{OC}} = \frac{\Delta S'_{\mathrm{OC}} \sigma'_{\mathrm{OC}}}{t'_{\mathrm{OC}}}, \tag{22}$$

and

$$\Delta S_{\mathrm{O,ir}} = \frac{Q_{\mathrm{O}}}{T_{\mathrm{O}}} - \Delta S_{\mathrm{O}} = \frac{\Delta S_{\mathrm{O}} \sigma_{\mathrm{O}}}{t_{\mathrm{O}}}. \tag{23}$$

It is necessary to impose the constraint $\sigma_{\mathrm{O}} = \sigma'_{\mathrm{OH}} + \sigma'_{\mathrm{OC}}$ in order to make the two different models have the same dissipation symmetry. Accordingly, it can be proved by using equations (5), (19), and (20) that $Q_{\mathrm{O}} = Q'_{\mathrm{OH}} + Q'_{\mathrm{OC}}$ and $\Delta S_{\mathrm{O,ir}} = \Delta S'_{\mathrm{OH,ir}} + \Delta S'_{\mathrm{OC,ir}}$ only if the condition

$$\frac{\sigma'_{\mathrm{OH}}}{t'_{\mathrm{OH}}} = \frac{\sigma'_{\mathrm{OC}}}{t'_{\mathrm{OC}}} = \frac{\sigma_{\mathrm{O}}}{t_{\mathrm{O}}} \tag{24}$$

is satisfied.

It can be realized from the above analyses that equation (24) is just the equivalent condition for the two low-dissipation models. In other cases, the two models are not equivalent any more. That is to say, the universal equivalence for the two different models under endoreversible assumption is invalid within the frame of low-dissipation assumption. In other words, the endoreversible assumption and the low-dissipation assumption lead to different conclusions in this scenario. This is another important achievement of the present paper, which means the equivalence between various finite-time thermodynamic models needs to be reevaluated in regard of multi-terminal systems.

Based on equations (15)–(24) and the above discussions, it can be further deduced that the equivalence between endoreversible combined and non-combined models is due to the

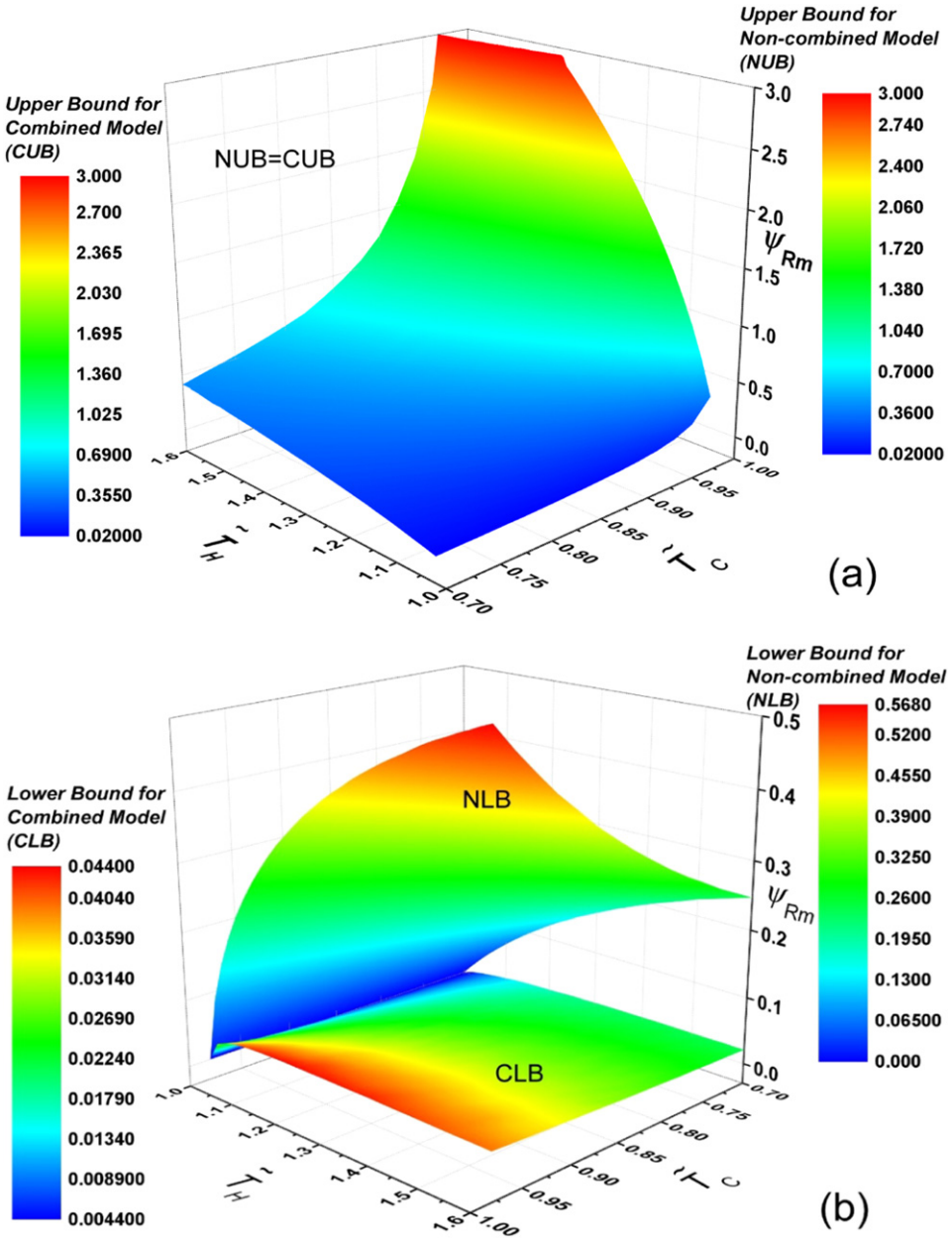

Figure 9. Three-dimensional graph of the upper (a) and lower bounds (b) of ψ_{Rm} for two different models of the three-terminal refrigerator.

linear relationship between the transferred heat and the heat transfer time duration. This linear relationship is no longer valid for the low-dissipation model. Consequently, the division of the time duration of the heat transfer process contacting with intermediate-temperature terminal results in different outcomes.

Moreover, the identical upper bounds and the striking distinctions for the lower bounds can be further explained based on the above analyses. When all the dissipation is generated from high-temperature terminal (i.e. $\tilde{\sigma}_{\mathrm{H}} \to 1$, $\tilde{\sigma}_{\mathrm{C}} \to 0$, and $\tilde{\sigma}_{\mathrm{O}} \to 0$), the condition shown by equation (24) can be satisfied. Hence, the identical upper bound of ψ_{Rm} can be obtained. By contrast, the minimum value of ψ_{Rm} for the combined model is attained when all the dissipation concentrates in the intermediate-temperature terminal [37] instead of low-temperature terminal (figure 6). In addition, due to the distinction of the irreversibility in the heat transfer processes contacting with the intermediate-temperature terminal, a new lower bound of ψ_{Rm} beneath the lower bound of ψ_{Rm} in figure 7 can be obtained as shown in figure 9(b). The detailed proofs are presented in appendix B.

It should be further pointed out that the low-dissipation non-combined model proposed in the present paper is more reasonable to be used to describe the various types of thermally driven refrigerators, mainly including absorption refrigeration, adsorption refrigeration, and ejector refrigeration. Because in the abovementioned thermally driven refrigerators, the involved working substance contacts with three heat reservoirs simultaneously rather than alternatingly. As a consequence, the more confined region limited by the obtained upper and lower bounds of CMP in the present paper is more reasonable as well. In contrast, the low-dissipation combined model depicted by figure 8 can be only used for the devices in which the working substance exchanges heat with three heat reservoirs by four heat transfer processes alternatingly.

It is worthy to mention that the proposed low-dissipation non-combined models and approaches can be further adopted to investigate the performance characteristics of other three-terminal devices, such as three-terminal heat pump, chemical pump, chemical potential transformer, etc.

7. Conclusions and prospects

In the present paper, a non-combined model of three-terminal refrigerator with fewer heat exchanging processes and the corresponding dissipation parameters has been proposed based on the low-dissipation assumptions. Most significant conclusions are underlined below:

(a) The performance characteristics of the low-dissipation three-terminal refrigerator has been investigated. Specially, the optimal relation between the COP and cooling power has been analytically derived, as shown by equation (14). The influences of size ratio and dissipation symmetry have been discussed. Besides, the optimal operating region $\psi_{Rm,A} < \psi < \psi_{\max,A}$ and size ratio $A_{\mathrm{r}} < A < A_{Rm}$ have been determined.

(b) According to the performance analyses, the three-dimensional upper and lower bounds of ψ_{Rm} varying with $\tilde{T}_{\mathrm{H}}$ and $\tilde{T}_{\mathrm{C}}$ have been obtained by setting $\tilde{\sigma}_{\mathrm{H}} \to 1$, $\tilde{\sigma}_{\mathrm{C}} \to 0$, $\tilde{\sigma}_{\mathrm{O}} \to 0$, and $\tilde{\sigma}_{\mathrm{H}} \to 0$, $\tilde{\sigma}_{\mathrm{C}} \to 1$, $\tilde{\sigma}_{\mathrm{O}} \to 0$ respectively, as shown by figure 7. In addition, the obtained bounds have been validated by comparing with the experimental and simulated results.

(c) The identical upper bounds and distinct lower bounds for the low-dissipation combined and non-combined models have been specially stressed by comparing the bounds of ψ_{Rm} obtained in the present paper and the results shown in reference [37]. Then, the claimed universal equivalence for the combined and non-combined models under endoreversible assumption [42, 43, 55] has been found to be invalid within the frame of low-dissipation assumption and the equivalence between various finite-time thermodynamic models needs to be reevaluated regarding multi-terminal systems.

(d) Attending the above distinction, the connection between the low-dissipation combined and non-combined models have been further revealed. The significant result is the

equivalent condition given by equation (24), according to which the identical upper bounds and distinct lower bounds of ψ_{Rm} have been theoretically demonstrated (as shown in appendix B).

(e) The low-dissipation non-combined model and the associated bounded region, shown in figures 1 and 7, respectively, are identified as the appropriate model and corrected bounded region for various types of thermally driven refrigerator by considering the differences between the combined and non-combined models and the operating mode of thermally driven refrigerators.

Finally, the proposed low-dissipation non-combined three-terminal model can be further used to investigate the performances of other three-terminal devices, such as three-terminal heat pump, chemical pump, chemical potential transformer, etc by using different trade-off figures of merit (e.g. Chi, Omega, and ecological functions). This could provide more comprehensive optimization criteria. Accordingly, the possible discussions for the stability [19, 28, 56] of various three-terminal devices may be further implemented by using the proposed model. In addition, the internal dissipation [18] and external leakage losses [57] can be further introduced to make the model more practical. Importantly, the conclusions of the present manuscript, namely, the inequivalence between combined and non-combined low-dissipation models and the appropriate model for describing the thermally driven refrigerator, may contribute to the further investigations on the equivalence between endoreversible and low-dissipation models for multi-terminal thermodynamic devices.

Acknowledgments

This work has been supported by the National Natural Science Foundation of China (Nos. 11405032 and 61773121). JGA thanks financial support for a postdoctoral contract from University of Salamanca under Program II. J Guo also thanks Professor Jincan Chen and Shanhe Su of Xiamen University for instructive discussions.

Data availability statement

The data that support the findings of this study are available upon reasonable request from the authors.

Appendix A. The expressions of A_i ($i = 1$–9) in equation (14)

Specific expressions of the parameters A_i appearing in equation (14),

$$A_1 = (A-1)J_1\left(AJ_2 + \sqrt{A}J_3\right), \tag{A1}$$

$$A_2 = (A-1)AJ_1J_2, \tag{A2}$$

$$A_3 = (A-1)(J_4+1)\left(AJ_2 + \sqrt{A}J_3\right), \tag{A3}$$

$$A_4 = (J_4+1)J_2A^2 - AJ_2J_4 + A\sqrt{A}(J_4+J_5+1)J_3, \tag{A4}$$

$$A_5 = (-1+A)^2 J_1^2, \tag{A5}$$

$$A_6 = (A-1)\,J_1\,[(1-A)\,(J_4+1)+J_4+AJ_5]\,, \tag{A6}$$

$$A_7 = (1-A)\,(J_4+1)\,(J_4+AJ_5), \tag{A7}$$

$$A_8 = AJ_1 + AJ_2 + 2\sqrt{A}J_3 + J_6, \tag{A8}$$

and

$$A_9 = AJ_5 + J_4. \tag{A9}$$

In equations (A1)–(A9), $J_1 = \tilde{\sigma}_{\rm C}\tilde{T}_{\rm C}$, $J_2 = \tilde{\sigma}_{\rm H}\tilde{T}_{\rm H}$, $J_3 = \sqrt{\tilde{\sigma}_{\rm H}\tilde{\sigma}_{\rm O}\tilde{T}_{\rm H}}$, $J_4 = \left(-1+\tilde{T}_{\rm C}\right)$, $J_5 = \left(\tilde{T}_{\rm H}-\tilde{T}_{\rm C}\right)$, and $J_6 = \tilde{\sigma}_{\rm O} - \tilde{\sigma}_{\rm C}\tilde{T}_{\rm C}$.

Appendix B. Demonstrations for identical upper bounds and distinct lower bounds

Here the theoretical analysis of the upper and lower bounds is addressed.

B.1. The demonstration for the identical upper bounds of the combined and non-combined models

For the combined low-dissipation model of three-terminal refrigerator proposed in reference [37] (figure 8), the upper bound of CMP are obtained by setting $\beta \to 1$, $\tilde{\sigma}'_{\rm C} \to 1$, and $\tilde{\sigma}'_{\rm H} \to 1$, where $\beta = (\sigma'_{\rm H}+\sigma'_{\rm OH})/(\sigma'_{\rm H}+\sigma'_{\rm OH}+\sigma'_{\rm OC}+\sigma'_{\rm C})$, $\tilde{\sigma}'_{\rm H} = \sigma'_{\rm H}/(\sigma'_{\rm H}+\sigma'_{\rm OH})$, and $\tilde{\sigma}'_{\rm C} = \sigma'_{\rm C}/(\sigma'_{\rm OC}+\sigma'_{\rm C})$ denoting the dissipation symmetry between two subsystems and the dissipation symmetry inside two subsystems respectively.

The optimal relations between the total time duration of Carnot heat engine subsystem $\tilde{\tau}'_{\rm he}$ ($\tilde{\tau}'_{\rm he} = \tilde{t}'_{\rm H} + \tilde{t}'_{\rm OH}$) and the partial time durations $\tilde{t}'_{\rm H}$ are given by [37]

$$\tilde{t}'_{\rm H} = \frac{\tilde{\sigma}'_{\rm H}\tilde{\tau}'_{\rm he} - \sqrt{\tilde{\sigma}'_{\rm H}\tilde{\tau}'_{\rm he}[\tilde{\tau}'_{\rm he} - (2\tilde{\sigma}'_{\rm H}-1)](1-\tilde{\sigma}'_{\rm H})}}{2\tilde{\sigma}'_{\rm H}-1}, \tag{B1}$$

where $\tilde{\tau}'_{\rm he} = \tau'_{\rm he}/(\sigma'_{\rm H}+\sigma'_{\rm OH})$, $\tilde{t}'_{\rm H} = t'_{\rm H}/(\sigma'_{\rm H}+\sigma'_{\rm OH})$, and $\tilde{t}'_{\rm OH} = t'_{\rm OH}/(\sigma'_{\rm H}+\sigma'_{\rm OH})$.

Similarly, the optimal relations between the total time duration of Carnot refrigerator subsystem $\tilde{\tau}'_{\rm re}$ ($\tilde{\tau}'_{\rm re} = \tilde{t}'_{\rm C} + \tilde{t}'_{\rm OC}$) and the partial time durations $\tilde{t}'_{\rm C}$ are expressed as [37]

$$\tilde{t}'_{\rm C} = \frac{\tilde{\sigma}'_{\rm C}\tilde{\tau}'_{\rm re} - \sqrt{\tilde{\sigma}'_{\rm C}\tilde{\tau}'_{\rm re}[\tilde{\tau}'_{\rm re} - (2\tilde{\sigma}'_{\rm C}-1)](1-\tilde{\sigma}'_{\rm C})}}{2\tilde{\sigma}'_{\rm C}-1}, \tag{B2}$$

where $\tilde{\tau}'_{\rm re} = \tau'_{\rm re}/(\sigma'_{\rm C}+\sigma'_{\rm OC})$, $\tilde{t}'_{\rm C} = t'_{\rm C}/(\sigma'_{\rm C}+\sigma'_{\rm OC})$, and $\tilde{t}'_{\rm OC} = t'_{\rm OC}/(\sigma'_{\rm C}+\sigma'_{\rm OC})$.

Accordingly, at the condition $\beta \to 1$, $\tilde{\sigma}'_{\rm C} \to 1$, and $\tilde{\sigma}'_{\rm H} \to 1$, one has

$$\frac{\sigma'_{\mathrm{OH}}}{\sigma'_{\mathrm{OC}}} = \frac{\tilde{\sigma}'_{\mathrm{OH}}}{\tilde{\sigma}'_{\mathrm{OC}}}\frac{\beta}{1-\beta} = \frac{1-\tilde{\sigma}'_{\mathrm{H}}}{1-\tilde{\sigma}'_{\mathrm{C}}}\frac{\beta}{1-\beta} \to \infty \tag{B3}$$

and

$$\begin{aligned}\frac{t'_{\mathrm{OH}}}{t'_{\mathrm{OC}}} &= \frac{\tilde{\tau}'_{\mathrm{he}} - \tilde{t}'_{\mathrm{H}}}{\tilde{\tau}'_{\mathrm{re}} - \tilde{t}'_{\mathrm{C}}}\frac{\beta}{1-\beta} \\ &= \frac{\tilde{\tau}'_{\mathrm{he}} - \frac{\tilde{\sigma}'_{\mathrm{H}}\tilde{\tau}'_{\mathrm{he}} - \sqrt{\tilde{\sigma}'_{\mathrm{H}}\tilde{\tau}'_{\mathrm{he}}[\tilde{\tau}'_{\mathrm{he}} - (2\tilde{\sigma}'_{\mathrm{H}} - 1)](1-\tilde{\sigma}'_{\mathrm{H}})}}{2\tilde{\sigma}'_{\mathrm{H}} - 1}}{\tilde{\tau}'_{\mathrm{re}} - \frac{\tilde{\sigma}'_{\mathrm{C}}\tilde{\tau}'_{\mathrm{re}} - \sqrt{\tilde{\sigma}'_{\mathrm{C}}\tilde{\tau}'_{\mathrm{re}}[\tilde{\tau}'_{\mathrm{re}} - (2\tilde{\sigma}'_{\mathrm{C}} - 1)](1-\tilde{\sigma}'_{\mathrm{C}})}}{2\tilde{\sigma}'_{\mathrm{C}} - 1}}\frac{\beta}{1-\beta} \to \frac{\tilde{\tau}'_{\mathrm{he}} - \tilde{\tau}'_{\mathrm{he}}}{\tilde{\tau}'_{\mathrm{re}} - \tilde{\tau}'_{\mathrm{re}}}\frac{\beta}{1-\beta} \to \infty,\end{aligned} \tag{B4}$$

where $\tilde{\sigma}'_{\mathrm{OH}} = \sigma'_{\mathrm{OH}}/(\sigma'_{\mathrm{H}} + \sigma'_{\mathrm{OH}})$, $\tilde{\sigma}'_{\mathrm{OC}} = \sigma'_{\mathrm{OC}}/(\sigma'_{\mathrm{OC}} + \sigma'_{\mathrm{C}})$. Combining equations (B3) and (B4) leads to the conclusion $\sigma'_{\mathrm{OH}}/\sigma'_{\mathrm{OC}} = t'_{\mathrm{OH}}/t'_{\mathrm{OC}}$, which indicates equation (24) is satisfied at the condition achieving the upper bound of CMP. In other words, the combined and non-combined model are equivalent at the condition of $\beta \to 1$, $\tilde{\sigma}'_{\mathrm{C}} \to 1$, and $\tilde{\sigma}'_{\mathrm{H}} \to 1$. Consequently, the identical upper bounds, as shown in figure 9(a), can be obtained.

B.2. The demonstration for the distinct lower bounds of the combined and non-combined models

Using the similar approach, at the condition attaining the lower bound of CMP for the combined model, i.e. $\beta \to 0$, $\tilde{\sigma}'_{\mathrm{C}} \to 0$, and $\tilde{\sigma}'_{\mathrm{H}} \to 0$, one can deduce

$$\frac{\sigma'_{\mathrm{OH}}}{\sigma'_{\mathrm{OC}}} = \frac{\tilde{\sigma}'_{\mathrm{OH}}}{\tilde{\sigma}'_{\mathrm{OC}}}\frac{\beta}{1-\beta} = \frac{1-\tilde{\sigma}'_{\mathrm{H}}}{1-\tilde{\sigma}'_{\mathrm{C}}}\frac{\beta}{1-\beta} \to 0 \tag{B5}$$

and

$$\begin{aligned}\frac{t'_{\mathrm{OH}}}{t'_{\mathrm{OC}}} &= \frac{\tilde{\tau}'_{\mathrm{he}} - \tilde{t}'_{\mathrm{H}}}{\tilde{\tau}'_{\mathrm{re}} - \tilde{t}'_{\mathrm{C}}}\frac{\beta}{1-\beta} \\ &= \frac{\tilde{\tau}'_{\mathrm{he}} - \frac{\tilde{\sigma}'_{\mathrm{H}}\tilde{\tau}'_{\mathrm{he}} - \sqrt{\tilde{\sigma}'_{\mathrm{H}}\tilde{\tau}'_{\mathrm{he}}[\tilde{\tau}'_{\mathrm{he}} - (2\tilde{\sigma}'_{\mathrm{H}} - 1)](1-\tilde{\sigma}'_{\mathrm{H}})}}{2\tilde{\sigma}'_{\mathrm{H}} - 1}}{\tilde{\tau}'_{\mathrm{re}} - \frac{\tilde{\sigma}'_{\mathrm{C}}\tilde{\tau}'_{\mathrm{re}} - \sqrt{\tilde{\sigma}'_{\mathrm{C}}\tilde{\tau}'_{\mathrm{re}}[\tilde{\tau}'_{\mathrm{re}} - (2\tilde{\sigma}'_{\mathrm{C}} - 1)](1-\tilde{\sigma}'_{\mathrm{C}})}}{2\tilde{\sigma}'_{\mathrm{C}} - 1}}\frac{\beta}{1-\beta} \to \frac{\tilde{\tau}'_{\mathrm{he}}}{\tilde{\tau}'_{\mathrm{re}}}\frac{\beta}{1-\beta} = \frac{\tau'_{\mathrm{he}}}{\tau'_{\mathrm{re}}} \to \infty\end{aligned} \tag{B6}$$

by considering the Carnot heat engine subsystem is operating close to reversible limit at $\beta \to 0$. According to equations (B5) and (B6), $\sigma'_{\mathrm{OH}}/\sigma'_{\mathrm{OC}} \neq t'_{\mathrm{OH}}/t'_{\mathrm{OC}}$. As a consequence, the equivalent condition, namely equation (24), is not satisfied at this condition and the distinct lower bounds are generated.

ORCID iDs

Hanxin Yang https://orcid.org/0000-0002-9642-9228
Juncheng Guo https://orcid.org/0000-0003-3397-1586

References

[1] Curzon F L and Ahlborn B 1975 *Am. J. Phys.* **43** 22
[2] Van den Broeck C 2005 *Phys. Rev. Lett.* **95** 190602

[3] Izumida Y and Okuda K 2012 *Europhys. Lett.* **97** 10004
[4] Izumida Y and Okuda K 2015 *New J. Phys.* **17** 085011
[5] Esposito M, Kawai R, Lindenberg K and Van den Broeck C 2010 *Phys. Rev. Lett.* **105** 150603
[6] Hu Y, Wu F, Ma Y, He J, Wang J, Hernández A C and Roco J M M 2013 *Phys. Rev.* E **88** 062115
[7] Guo J, Wang J, Wang Y and Chen J 2013 *Phys. Rev.* E **87** 012133
[8] Abiuso P and Perarnau-Llobet M 2020 *Phys. Rev. Lett.* **124** 110606
[9] Wang R, Wang J, He J and Ma Y 2013 *Phys. Rev.* E **87** 042119
[10] Guo J, Wang Y and Chen J 2012 *J. Appl. Phys.* **112** 103504
[11] Wang Y, Li M, Tu Z C, Hernández A C and Roco J M M 2012 *Phys. Rev.* E **86** 011127
[12] de Tomás C, Roco J M M, Hernández A C, Wang Y and Tu Z C 2013 *Phys. Rev.* E **87** 012105
[13] Hernández A C, Medina A and Roco J M M 2015 *New J. Phys.* **17** 075011
[14] de Tomás C, Hernández A C and Roco J M M 2012 *Phys. Rev.* E **85** 010104(R)
[15] Ma Y H, Zhai R X, Chen J, Sun C P and Dong H 2020 *Phys. Rev. Lett.* **125** 210601
[16] Gonzalez-Ayala J, Medina A, Roco J M M and Hernández A C 2018 *Phys. Rev.* E **97** 022139
[17] Du J, Shen W, Zhang X, Su S and Chen J 2020 *Phys. Rev. Res.* **2** 013259
[18] Wang J and He J 2012 *Phys. Rev.* E **86** 051112
[19] Reyes-Ramírez I, Gonzalez-Ayala J, Hernández A C and Santillán M 2017 *Phys. Rev.* E **96** 042128
[20] Ma Y H, Xu D, Dong H and Sun C P 2018 *Phys. Rev.* E **98** 042112
[21] Holubec V and Ryabov A 2016 *J. Stat. Mech.* 073204
[22] Singh V and Johal R S 2018 *Phys. Rev.* E **98** 062132
[23] Holubec V and Ye Z 2020 *Phys. Rev.* E **101** 052124
[24] Gonzalez-Ayala J, Hernández A C and Roco J M M 2016 *J. Stat. Mech.* 073202
[25] Hernández A C, Medina A, Roco J M M, White J A and Velasco S 2001 *Phys. Rev.* E **63** 037102
[26] Long R, Liu Z and Liu W 2014 *Phys. Rev.* E **89** 062119
[27] Gonzalez-Ayala J, Hernández A C and Roco J M M 2017 *Phys. Rev.* E **95** 022131
[28] Gonzalez-Ayala J, Guo J, Medina A, Roco J M M and Hernández A C 2019 *Phys. Rev.* E **100** 062128
[29] Izumida Y, Okuda K, Roco J M M and Hernández A C 2015 *Phys. Rev.* E **91** 052140
[30] Zhang Y and Huang Y 2020 *Phys. Rev.* E **102** 012151
[31] Johal R S 2017 *Phys. Rev.* E **96** 012151
[32] Gonzalez-Ayala J, Roco J M M, Medina A and Hernández A C 2017 *Entropy* **19** 182
[33] Wang F, Zhao J, Zhang H, Miao H, Zhao J, Wang J, Yuan J and Yan J 2018 *Appl. Energy* **230** 267
[34] Said S A M, El-Shaarawi M A I and Siddiqui M U 2012 *Int. J. Refrig.* **35** 1967
[35] Peng W, Ye Z, Zhang X and Chen J 2018 *Energy Convers. Manage.* **166** 74
[36] Erdman P A, Bhandari B, Fazio R, Pekola J P and Taddei F 2018 *Phys. Rev.* B **98** 045433
[37] Guo J, Yang H, Zhang H, Gonzalez-Ayala J, Roco J M M, Medina A and Hernández A C 2019 *Energy Convers. Manage.* **198** 111917
[38] Ye Z and Holubec V 2021 *Phys. Rev.* E **103** 052125
[39] Huang F F 1976 *Engineering Thermodynamics* (London: Macmillan)
[40] Su S, Chen J F, Ma Y, Chen J and Sun C 2018 *Chin. Phys.* B **27** 060502
[41] Cavina V, Mari A and Giovannetti V 2017 *Phys. Rev. Lett.* **119** 050601
[42] Yan Z and Chen J 1989 *J. Appl. Phys.* **65** 1
[43] Chen J and Wu C 1996 *Appl. Therm. Eng.* **16** 901
[44] Chen J 1997 *J. Phys. D: Appl. Phys.* **30** 582
[45] Boudéhenn F, Demasles H, Wyttenbach J, Jobard X, Chèze D and Papillon P 2012 *Energy Proc.* **30** 35
[46] Darwish N A, Al-Hashimi S H and Al-Mansoori A S 2008 *Int. J. Refrig.* **31** 1214
[47] Wang X L, Chua H T and Ng K C 2005 *Int. J. Refrig.* **28** 756
[48] Oliveira R G, Silveira V Jr and Wang R Z 2006 *Appl. Therm. Eng.* **26** 303
[49] Gong L X, Wang R Z, Xia Z Z and Chen C J 2011 *Energy Convers. Manage.* **52** 2345
[50] Amar N B, Sun L M and Meunier F 1996 *Appl. Therm. Eng.* **16** 405
[51] Nguyen V M, Riffat S B and Doherty P S 2001 *Appl. Therm. Eng.* **21** 157
[52] Shen S, Qu X, Zhang B, Riffat S and Gillott M 2005 *Appl. Therm. Eng.* **25** 2891
[53] Kasperski J and Gil B 2014 *Appl. Therm. Eng.* **71** 197
[54] Wang J H, Wu J H, Hu S S and Huang B J 2009 *Appl. Therm. Eng.* **29** 1904
[55] Chen J and Yan Z 1989 *J. Chem. Phys.* **90** 4951
[56] Gonzalez-Ayala J, Guo J, Medina A, Roco J M M and Calvo Hernández A 2020 *Phys. Rev. Lett.* **124** 050603
[57] Huang C, Guo J and Chen J 2015 *Chin. Phys.* B **24** 110506